



FULL PAPER

Pathology

Rat polyomavirus 2 infection in a colony of X-linked severe combined immunodeficiency rats in Japan

Miyuu TANAKA^{1,2)}, Mizuki KURAMOCHI²⁾, Satoshi NAKANISHI¹⁾,
Mitsuru KUWAMURA²⁾ and Takashi KURAMOTO^{1,3)*}

¹⁾Institute of Laboratory Animals, Graduate School of Medicine, Kyoto University, Yoshidakonoe-cho, Sakyo-ku, Kyoto 606-8501, Japan

²⁾Laboratory of Veterinary Pathology, Graduate School of Life and Environmental Science, Osaka Prefecture University, Rinkuu Ourai Kita 1-58, Izumisano, Osaka 598-8531, Japan

³⁾Current address: Department of Animal Science, Faculty of Agriculture, Tokyo University of Agriculture, 1737 Funako, Atsugi, Kanagawa 243-0034, Japan

ABSTRACT. Polyomaviruses (PyVs) infect a wide range of animals and provoke wasting diseases, particularly in immunosuppressed hosts. Recently, a novel *Rattus norvegicus* polyomavirus 2 (RatPyV2) has been identified in a colony of X-linked severe combined immunodeficiency (X-SCID) rats in the United States. Here, we describe the first report of the RatPyV2 infection in an X-SCID rat colony in Japan. The affected rats exhibited adult-onset wasting. Histologically, we observed large basophilic intranuclear inclusion bodies within the hyperplastic or dysplastic epithelial cells in the salivary glands, Harderian glands, extraorbital lacrimal glands, and in respiratory and reproductive tissues. Among these organs, the parotid salivary, Harderian, and extraorbital lacrimal glands were most obviously affected. In particular, the parotid salivary glands were the most severely and diffusely affected and atrophic lesions were prominent even at 1 month of age, which suggested that the parotid salivary glands would be highly susceptible to RatPyV2 in X-SCID rats. RatPyV2 inclusion bodies were also detected in the tail of the epididymis and deferent duct. Such reproductive lesions developed significantly in the later stage of breeding age, and therefore may be associated with the reduced fecundity observed in the infected X-SCID rats. We also established a simple, rapid, and non-invasive diagnostic method based on the Amp-FTA method, using buccal swabs for the detection of RatPyV2 in immunodeficient rats. Our findings contribute to the early detection and diagnosis of RatPyV2 infections.

KEY WORDS: Amp-FTA, intranuclear inclusion body, *Rattus norvegicus* polyomavirus 2, salivary gland, X-SCID rat

J. Vet. Med. Sci.

80(9): 1400–1406, 2018

doi: 10.1292/jvms.18-0107

Received: 4 March 2018

Accepted: 5 July 2018

Published online in J-STAGE:
16 July 2018

Polyomaviruses are a family of non-enveloped icosahedral DNA viruses that infect a variety of mammals, birds, marine fish, and insects. Most mammalian polyomaviruses cause latent subclinical infections [3, 10]. In humans, some immunosuppressed patients develop polyomavirus-associated diseases such as nephritis (BK virus), progressive multifocal leukoencephalopathy (JC virus), pneumonia (Washington University virus; WUPyV), and Merkel cell carcinoma (Merkel cell polyomavirus) [3, 5]. In laboratory mice, polyomaviruses cause tumor formation (Murine polyomavirus) and pneumonia (Murine pneumotropic virus) in immunodeficient mice or experimentally-inoculated newborn mice [5, 9, 13]. The prevalence of polyomavirus infection is considered to be quite low in contemporary mouse colonies [13].

In rats, *Rattus norvegicus* polyomavirus 1 (RnorPyV1), detected in feral Norway rats, was genetically characterized for the first time in 2015, although the infected rats were asymptomatic [6, 10]. Polyomavirus-associated diseases in rats were reported in athymic nude (NIH-*Foxn1*^{nu}) rats [7, 14, 16]. Infected nude rats developed a wasting disease with sialadenitis and/or pneumonia. Intranuclear inclusion bodies were present within the ductal and glandular epithelium in the salivary, Harderian, and laryngeal glands, and bronchi. Based on virus morphology and its immunoreactivity to the antibody to simian virus 40 (SV40), belonging to the *Betapolyomaviridae* genus [4], this virus was determined to be a polyomavirus [16]. Recently, a novel *Rattus norvegicus* polyomavirus 2 (RatPyV2) has been identified in a colony of X-linked severe combined immunodeficiency (X-SCID) rats lacking the interleukin-2 receptor gamma (*Il2rg*) gene in the United States [15]. Infected X-SCID rats showed adult-onset wasting, decreased fecundity, and/or dyspnea, and histopathological examination revealed inflammation, epithelial hyperplasia/dysplasia,

*Correspondence to: Kuramoto, T.: tk206782@nodai.ac.jp

©2018 The Japanese Society of Veterinary Science



This is an open-access article distributed under the terms of the Creative Commons Attribution Non-Commercial No Derivatives (by-nc-nd) License. (CC-BY-NC-ND 4.0: <https://creativecommons.org/licenses/by-nc-nd/4.0/>)

and intranuclear inclusion bodies in multiple epithelial sites including the salivary glands, Harderian glands, and respiratory and reproductive tissues.

In 2015, a 6.5-month-old female X-SCID rat from a rat colony of Kyoto University exhibited severe dyspnea and wasting. This rat was euthanized, and its lungs were collected for histopathology and microbial examination for *Pneumocystis carinii* (*P. carinii*). The affected rat was negative for *P. carinii* in pathological, serological, and PCR examination. However, we detected large basophilic intranuclear inclusions in the lung epithelium, suggesting polyomavirus infection.

In the present study, we conducted further necropsy examination of both premature and aged X-SCID rats to reveal detailed pathology and highly susceptible target tissues. We also established a simple and rapid diagnostic method to detect RatPyV2 using buccal swab samples in immunodeficient rat strains.

MATERIALS AND METHODS

Animals

X-SCID and F344/NSlc (Japan SLC, Inc., Shizuoka, Japan) rats were maintained at the Institute of Laboratory Animals, Graduate School of Medicine, Kyoto University. All animal experiments were approved by the Animal Research Committees of Kyoto University (MedKyo 17536) and were conducted according to the regulations on animal experimentation of Kyoto University.

Histopathology and transmission electron microscopy (TEM)

Rats were euthanized under isoflurane anesthesia. Tissues collected from 1- to 8.5-month-old X-SCID rats (n=23) were fixed in 10% neutral buffered formalin, and embedded in paraffin. The following tissues were sampled: liver, spleen, kidneys, heart, lungs, thymus, salivary glands, exorbital lacrimal glands, Harderian glands, testes, deferent ducts, epididymis, prostate glands, uterus, ovaries, and oviducts. Four μm -thick sections were cut and stained with hematoxylin and eosin (HE). Formalin-fixed tissues were also stored in 2.5% glutaraldehyde in 0.1 M phosphate buffer (PB; pH 7.4), post-fixed with 1% osmic tetroxide at 4°C overnight, and embedded in epoxy resin. Ultrathin sections were stained with uranyl acetate and lead citrate, and examined in a Hitachi H-7500 electron microscope (Hitachi, Tokyo, Japan).

Immunohistochemistry

For immunohistochemistry, paraffin-embedded tissue sections were dewaxed and pretreated in a microwave with Tris-EDTA buffer (pH 9.0) for 15 min. Sections were then incubated for 1 hr at room temperature with mouse anti-SV40 T antigen antibody (clone PAb416, 1:1,500; Millipore, Billerica, MA, U.S.A.). Horseradish peroxidase-conjugated polymer (Histofine Simple Stain MAX PO; Nichirei, Tokyo, Japan) was used as a secondary antibody. Signals were visualized with 3,3'-diaminobenzidine (DAB Substrate Kit; Nichirei).

PCR for RatPyV2 and sequence analysis

Genomic DNA was extracted from formalin-fixed paraffin-embedded (FFPE) sections (lung and salivary gland tissues) and feces, using NucleoSpin DNA FFPE XS and NucleoSpin DNA Stool (MACHEREY-NAGEL, Düren, Germany). PCR reactions (35 to 37 cycles) using primers for the β -actin and RatPyV2 virus protein 1 (VP1) were performed as described previously [15]. Sequencing of a larger region of VP1 (primer pair F14-R7, 432-bp [15]) was performed by MacroGen Japan Corp. (Kyoto, Japan).

For buccal swabs, direct PCR amplification by the Amp-FTA method was conducted [12]. Briefly, buccal swabs were collected with 4N6 FLOQSwabs (Copan, Brescia, Italy) and immediately smeared on the Whatman Indicating FTA Card (GE Healthcare, Little Chalfont, U.K.). Discs (1.5 mm diameter) were punched out from the FTA card by a standard ear punch and were directly used as templates (one disc for each reaction). PCR reactions (40 cycles) using primers for β -actin and RatPyV2 VP1 [15] were performed in Ampdirect Plus buffer (Shimadzu Corp., Kyoto, Japan). As a negative control, we used immunocompetent F344/NSlc strains that were negative for RatPyV2 serological assay, as conducted by IDEXX BioResearch (Columbia, MO, U.S.A.).

RESULTS

Clinical symptoms of RatPyV2 infected X-SCID rats

X-SCID rats exhibited adult-onset wasting and reduced fecundity, and affected rats showed high mortality after 6 months of age. Clinical symptoms included dyspnea, emaciation, low fecundity, and chromodacryorrhea that ranged from mild to severe (Supplemental Table 1). Although the fertility rate was 85.7% and the average number of pups per litter was 8.94, female X-SCID rats rarely had second or third litters, which indicated that the fecundity rate seemed to decrease after 3 or 4 months of age.

Pathology of RatPyV2 infection

At necropsy, mild to severe atrophy of the salivary glands (the parotid, submandibular, and sublingual glands), Harderian glands, and exorbital lacrimal glands was observed. The parotid salivary glands and Harderian glands were severely affected even at 1 to 2 months of age. In aged X-SCID rats with respiratory distress, lungs were mottled red or pink and showed varying degrees of red consolidation.

Histopathologically, multiple organs were affected; the salivary glands, Harderian glands, extraorbital lacrimal glands, and the

respiratory system as well as the reproductive organs (Table 1). The most characteristic finding was basophilic or amphophilic large intranuclear inclusion bodies within the hyperplastic or dysplastic epithelial cells (Fig. 1). Inclusion bodies showed various appearances; dense homogeneous, glassy, or pale granular, with or without a halo. Infected epithelial cells could be detected by immunohistochemistry for anti-SV40 (PAb416) antibody as previously reported (Figs. 1G and 2B) [2, 15].

In the salivary, Harderian, and extraorbital lacrimal glands, we observed severe loss, degeneration, or necrosis of acinar and ductal epithelia with mononuclear cell infiltration (Fig. 1A–D). The remaining epithelial components were hyperplastic, dysplastic, or disorganized. In advanced lesions, tissues were severely atrophied with areas of interstitial fibrosis and inflammation (Fig. 1B and 1D). There were many intranuclear inclusion bodies with halos (Fig. 1; black arrowheads) as well as full-type inclusion bodies in both acinar and ductal epithelial cells (Fig. 1; yellow arrowheads).

Among salivary glands, parotid salivary glands were the most severely and diffusely affected (Fig. 1A and 1B). Diffuse atrophic lesions were prominent from at least 1 month of age (Fig. 1A). In the submandibular salivary glands, moderate multifocal to locally extensive lesions appeared starting at around 3 months of age. Meanwhile, the sublingual and lingual salivary glands, which consisted of mucinous glands, were rarely affected. In these tissues, mild focal to multifocal lesions were observed starting at 7 months of age (Table 1).

In the Harderian glands, epithelial hyperplasia and dysplasia, and glandular atrophy were observed from at least 2.5 months of age (Fig. 1C). After 6 months of age, the Harderian glands were almost completely replaced with fibrotic tissue and disorganized or dilated glands (Fig. 1D).

In the extraorbital lacrimal glands, a few SV40-positive cells were detected in focal inflammatory areas starting at 1 month of age, although intranuclear inclusion bodies were not observed. Karyomegaly appeared in inflammatory foci and glandular atrophic lesions from 2 months of age in both sexes. Focal or multi-focal lesions could be detected from around 3 months of age (Table 1).

In the lungs, bronchiolar hyperplasia with atypia and large basophilic intranuclear inclusion bodies (full type) were identified starting at 1 month of age (Fig. 1E). Inclusion bodies were mainly located at the apical side of respiratory epithelial cells. In affected aged rats, inclusion bodies as well as karyomegaly were also detected in pneumocytes (Fig. 1F; 7 months of age), and interstitial pneumonia was present. On TEM examination of lung tissue, numerous icosahedral virus particles, 40 to 50 nm in diameter, were detected in the nuclei of the bronchial epithelial cells (Fig. 1H).

The uterus and prostate gland were also affected as previously described [1, 14]. We also detected intranuclear inclusion bodies or karyomegaly in the epithelial cells of the deferent ducts and the tail of the epididymis (Fig. 2). These reproductive organs showed significant lesions from around 6 months of age, although any apparent inclusion bodies were not observed before about 4 months of age.

Detection of RatPyV2 by PCR

We detected RatPyV2 VP1 products in all DNA samples extracted from feces and FFPE tissues of X-SCID rats, but not from the immunocompetent F344 strains (Fig. 3A). The sequences of the 432-bp VP1 fragment showed a 99–100% match with those of RatPyV2 (GenBank accession No. KX574453 and KX808699). We also detected single nucleotide polymorphisms (SNPs) at nucleotide positions 2085 (A/G) and 2092 (A/C) that were identical with those previously reported by Rigatti *et al.* [14] (Fig. 3B). The Amp-FTA method using buccal swabs detected RatPyV2 VP1 products in X-SCID rats by this method starting at around 1 month of age (Fig. 4).

DISCUSSION

In this study, we confirmed that the histological lesions observed in the X-SCID rats in Kyoto University were similar to those reported previously and that the VP1 DNA sequences were identical with those found in the United States [15]. Moreover, PCR analyses revealed that all of the X-SCID rats examined (n=25) were positive for RatPyV2, which suggests that the prevalence of RatPyV2 in the X-SCID rat colony was significantly high. The X-SCID rats that were involved in the outbreak in the United States were obtained from Kyoto University in June 2015 [15]. Thus, these findings suggest that the RatPyV2-infected X-SCID rats were shipped to the U.S.A. rather than having become infected with RatPyV2 during or after shipping.

Previous pathological analyses demonstrated that epithelial hyperplasia and dysplasia of the salivary glands, Harderian glands, and lungs were characteristic in the RatPyV2-infected X-SCID rats. Glandular atrophy and loss in the salivary and Harderian glands were also characteristic [15]. These pathological characteristics were confirmed in the X-SCID rats used in this study. In addition, we found that the severity of the histological lesions varied among organs. Specifically, the parotid salivary glands and extraorbital lacrimal glands were affected as early as 1 month of age, and the Harderian gland lesions developed between 1 to 2 months of age. Therefore, we considered that the parotid salivary and extraorbital lacrimal glands were the most highly susceptible to RatPyV2 in X-SCID rats.

Intranuclear inclusion bodies were present in the salivary glands, lacrimal glands, and lung at 1 month of age, which strongly suggested that viral transmission occurred at least one week after the weaning. As intranuclear inclusion bodies were prominent in the epithelia of active mammary glands and the uterus [15], it is likely that X-SCID fetuses would be exposed to RatPyV2 in utero and that direct contact with oral, nasal, or respiratory secretions would largely contribute to RatPyV2 infection.

In laboratory rats, karyomegaly is often observed in the lacrimal gland. These lesions are predominantly found in male rats and are age-related [8]. Our histological study showed that karyomegaly was observed in both male and female rats starting at 2–3 months of age. Although it is necessary to distinguish these lesions from pseudoinclusions, it is likely that karyomegaly

Table 1. Histopathologic lesions in RatPyV2 infected rats in this study

	Age and number of rats (M: male, F: female)	1 month of age 3 (M:2, F:1)	2–3 months of age 9 (M:7, F:2)	4–5 months of age 6 (M:4, F:2)	>6 months of age 7 (M:3, F:4)
Parotid salivary glands	Intranuclear inclusion bodies	Present ^{a)}	Present ^{a)}	Present ^{a)}	Present ^{a)}
	Epithelial hyperplasia and dysplasia	Diffuse, moderate	Diffuse, moderate to severe	Diffuse, severe	Diffuse, severe
	Glandular atrophy, loss, and necrosis	Diffuse, moderate	Diffuse, moderate to severe	Diffuse, severe	Diffuse, severe
	Mononuclear cell infiltration	Diffuse, moderate to severe	Diffuse, moderate to severe	Diffuse, moderate to severe	Diffuse, moderate to severe
	Fibrosis	Mild	Diffuse, moderate	Diffuse, moderate to severe	Diffuse, severe
Submandibular glands	Intranuclear inclusion bodies	—	Present ^{a)}	Present ^{a)}	Present ^{a)}
	Epithelial hyperplasia and dysplasia	—	Multi-focal, mild	Multi-focal to locally extensive, moderate	Multi-focal to locally extensive, moderate
	Glandular atrophy, loss, and necrosis	—	Multi-focal, mild	Multi-focal to locally extensive, moderate	Multi-focal to locally extensive, moderate
	Mononuclear cell infiltration	—	Multi-focal, mild	Multi-focal to locally extensive, moderate	Multi-focal to locally extensive, moderate
	Fibrosis	—	—	Mild	Mild
Sublingual glands	Intranuclear inclusion bodies	—	Present ^{a)}	Present ^{a)}	Present ^{a)}
	Epithelial hyperplasia and dysplasia	—	Focal, mild	Focal to multi-focal, mild	Focal to multi-focal, mild
	Glandular atrophy and loss	—	—	—	—
	Mononuclear cell infiltration	—	—	Focal to multi-focal, mild	Focal to multi-focal, mild
	Fibrosis	—	—	—	—
Harderian glands	Intranuclear inclusion bodies	—	Present ^{a)}	Present ^{a)}	Present ^{a)}
	Epithelial hyperplasia and dysplasia	—	Multi-focal, moderate	Diffuse, moderate to severe	Diffuse, severe
	Glandular atrophy, loss, and necrosis	—	Multi-focal, moderate	Diffuse, moderate to severe	Diffuse, severe
	Mononuclear cell infiltration	—	Multi-focal, moderate	Diffuse, moderate to severe	Diffuse, moderate to severe
	Fibrosis	—	Mild	Diffuse, moderate	Diffuse, severe
Extraorbital lacrimal glands	Intranuclear inclusion bodies	— ^{a)}	Present ^{a)}	Present ^{a)}	Present ^{a)}
	Mononuclear cell infiltration	Focal, mild to moderate	Focal to multi-focal, moderate	Multi-focal, moderate	Multi-focal, moderate to severe
	Glandular atrophy and loss	—	Focal to multi-focal, mild to moderate	Multi-focal, moderate	Diffuse, moderate to severe
	Karyomegaly	—	Present ^{a)}	Present ^{a)}	Present ^{a)}
	Fibrosis	—	—	—	—
Lung	Bronchiolar intranuclear inclusion bodies	Present ^{a)}	Present ^{a)}	Present ^{a)}	Present ^{a)}
	Alveolar intranuclear inclusion bodies	—	—	—	—
	Bronchiolar hyperplasia	Mild to moderate	Moderate	Moderate	Moderate
	Interstitial pneumonia	Mild to moderate	Mild to moderate	Moderate	Severe
	Fibrosis	—	—	—	—
Prostate glands	Intranuclear inclusion bodies	—	—	Present ^{a)}	Present ^{a)}
	Epithelial hyperplasia and dysplasia	—	—	Moderate	Severe
	Glandular atrophy and degeneration	—	—	Mild to moderate	Severe
	Intranuclear inclusion bodies	—	—	—	—
	Fibrosis	—	—	—	—
Deferent ducts	Intranuclear inclusion bodies	—	—	—	—
	Epithelial hyperplasia and dysplasia	—	—	—	—
	Glandular atrophy and degeneration	—	—	—	—
	Intranuclear inclusion bodies	—	—	—	—
	Fibrosis	—	—	—	—
Epididymis	Intranuclear inclusion bodies	—	—	—	—
	Epithelial hyperplasia and dysplasia	—	—	—	—
	Glandular atrophy and degeneration	—	—	—	—
	Intranuclear inclusion bodies	—	—	—	—
	Fibrosis	—	—	—	—
Uterus	Intranuclear inclusion bodies	—	—	—	—
	Epithelial hyperplasia and dysplasia	—	—	—	—
	Glandular atrophy and degeneration	—	—	—	—
	Intranuclear inclusion bodies	—	—	—	—
	Fibrosis	—	—	—	—

—: Lesions were not detected. a) SV40 positive cells were detected by immunohistochemistry.

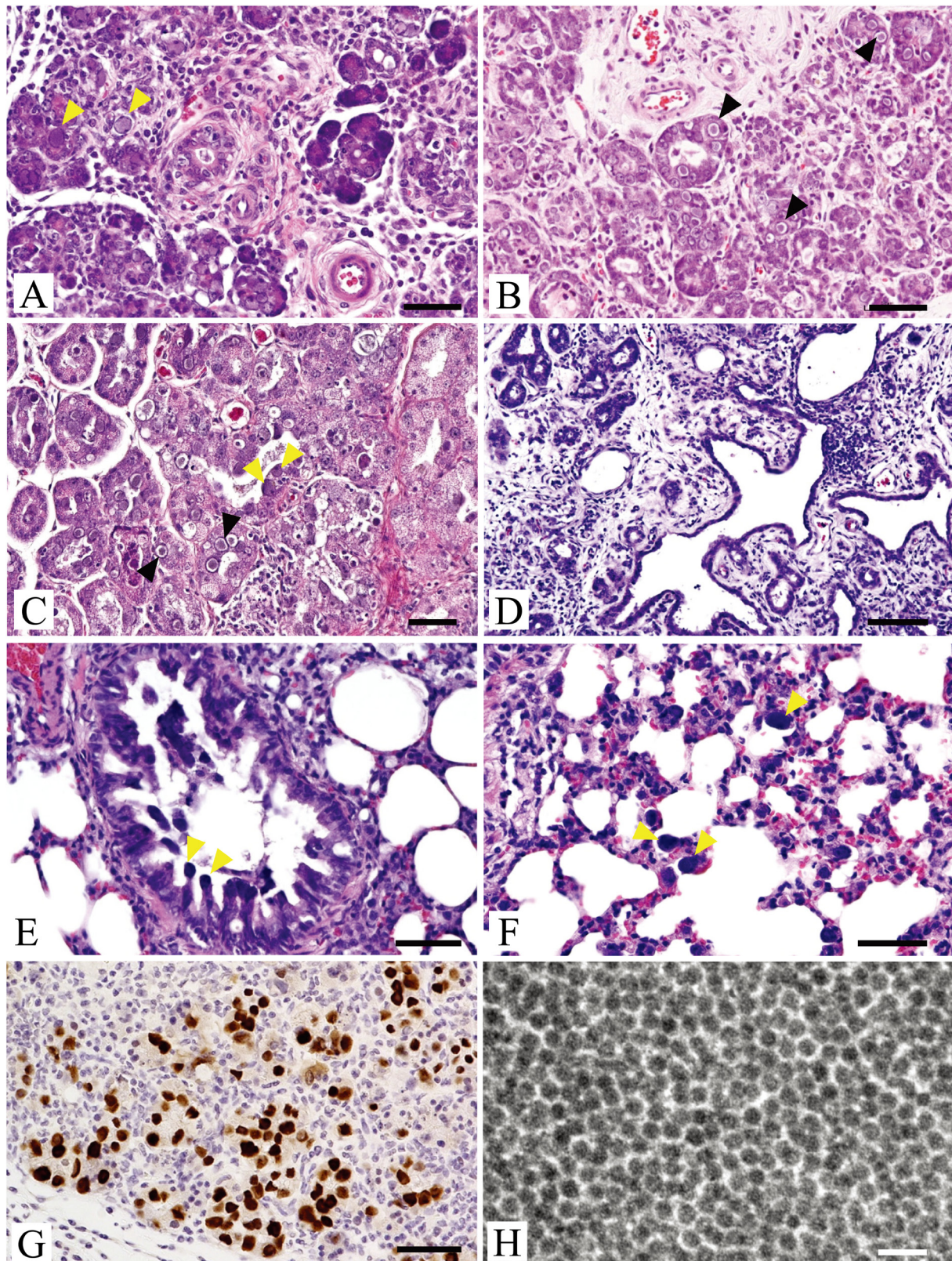


Fig. 1. Histopathology of affected organs of X-SCID rats. Intranuclear inclusion bodies with (black arrowheads) or without (yellow arrowheads) a halo are evident. (A) Parotid salivary gland, 1 month of age; (B) Parotid salivary gland, 7 months of age; (C) Harderian gland, 2.5 months of age; (D) Harderian gland, 7 months of age; (E) Lung, 1 month of age; and (F) Pulmonary alveoli, 7 months of age. (G) Immunohistochemistry for SV40 T antigen (PAb416). Parotid salivary gland, 1 month of age. (H) Transmission electron microscopy image of lung. Numerous virus particles in the bronchial epithelial cell. The virus particles show icosahedral shape and are 40 to 50 nm in diameter. Bar=50 μ m (A–C and E–G), 100 μ m (D), and 100 nm (H).

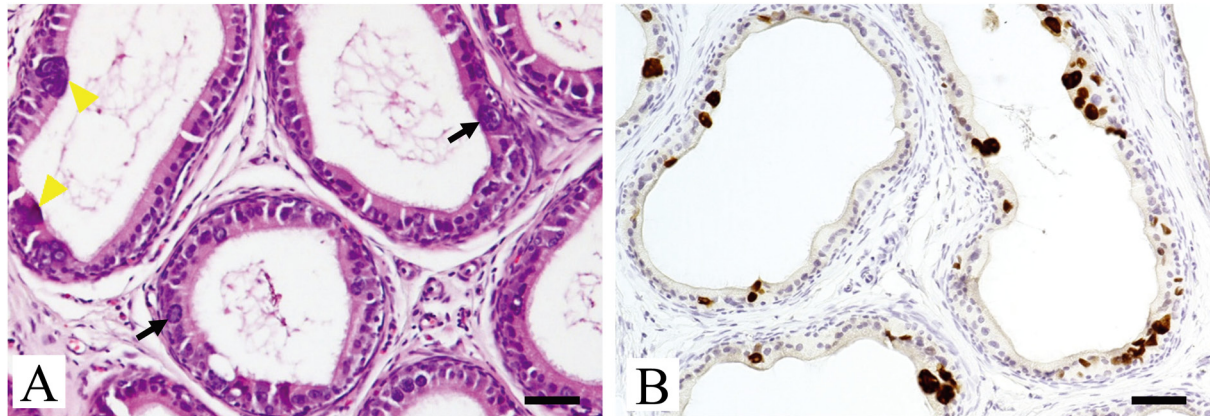


Fig. 2. Pathological analyses of the epididymis. (A) Histopathology of the 7-month-old-X-SCID rat. Intranuclear inclusion bodies (yellow arrowheads) and large atypical nuclei (arrows) are observed. (B) Immunohistochemistry for SV40 T antigen on the epididymis of a 7-month-old X-SCID rat. Intranuclear inclusion bodies are immunopositive for SV40 T antigen. Bar=50 μ m.

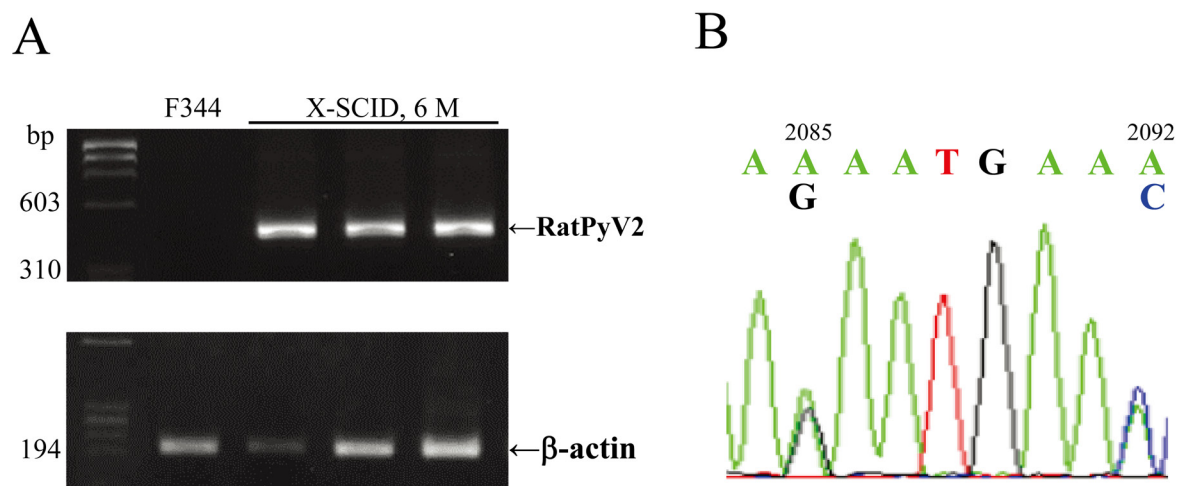


Fig. 3. Detection of RatPyV2 DNA by PCR and sequence analysis. (A) PCR amplification from feces. RatPyV2 VP1 products (432 bp) are detected from X-SCID rats but not immunocompetent F344 rats. β -actin (191 bp) is used as an internal control. (B) Two SNPs at nucleotide position 2085 (A/G) and 2092 (A/C) are detected in the RatPyV2 VP1 region.

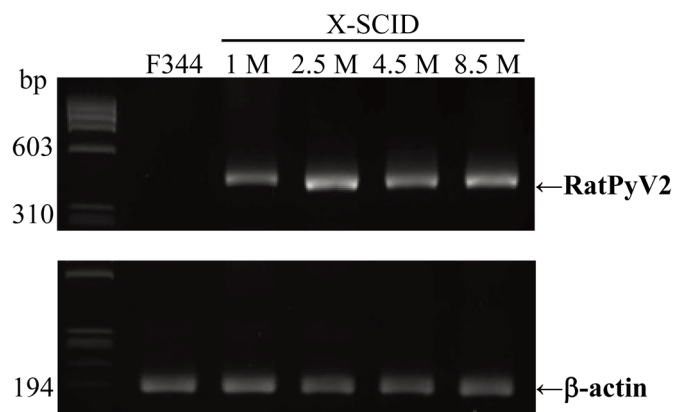


Fig. 4. Detection of RatPyV2 DNA from buccal swabs by the Amp-FTA method. RatPyV2 VP1 products (432 bp) are detected even in 1-month-old X-SCID rats. β -actin (191 bp) is used as an internal control.

resulted from RatPyV2 infection.

Several PyVs have been reported to be involved in tumor development that is mediated by tumor antigens [5]. The RatPyV2 genome encodes the open reading frame for large T antigen [15]. Some PyV large T antigens, such as SV40 large T antigen, are oncoproteins that can induce neoplastic transformation in the host cell [1]. We observed no neoplastic lesions, but did observe hyperplastic and dysplastic changes with atypical or karyomegaly cells in the affected atrophic organs of the RatPyV2-infected X-SCID rats. We could not eliminate the possibility that these hyperplastic and dysplastic changes may be the result of RatPyV2 infection. Further investigation would clarify the involvement of RatPyV2 in hyperplastic and dysplastic cellular changes.

In the present study, we established a rapid, simple, and non-invasive diagnostic method based on the Amp-FTA method using buccal swabs [11]. This method could detect RatPyV2 infection in our X-SCID rat colony. FTA discs could be directly used as PCR templates and therefore the purification of DNA was not required. In addition, the buccal swabs were suitable starting materials, because the salivary glands were highly susceptible to RatPyV2. Indeed, this method allowed us to detect the RatPyV2 gene in X-SCID rats as early as 1 month of age. Thus, we recommend the Amp-FTA method using buccal swabs for the early detection of RatPyV2 in colonies of immunodeficient rats.

A serological survey for RatPyV2 among immunocompetent rats in North America revealed that 32% of samples were positive for the anti-RatPyV2 antibody, which suggested widespread RatPyV2 infection in laboratory rat populations [2]. At this time, a serological test for RatPyV2 is only available from IDEXX BioResearch in the United States. Therefore, we are planning to evaluate the utility of the Amp-FTA method using buccal swabs for detecting RatPyV2-infected immunocompetent rats.

In summary, we have been the first to detect the RatPyV2 infection in a colony of X-SCID rats in Japan. Our histological examination strongly suggested that the parotid salivary glands and extraorbital lacrimal glands were the most highly susceptible tissue to RatPyV2. The Amp-FTA method using buccal swabs is useful for the rapid antemortem diagnosis of RatPyV2 in immunodeficient rats.

ACKNOWLEDGMENTS. We wish to thank the National Bio Resource Project–Rat in Japan (<http://www.anim.med.kyoto-u.ac.jp/NBR/>) for providing F344-*Il2rg^{em7Kyo}* rats (NBRP Rat No. 0694). We are also grateful to K. Yamasaki, Y. Neoda, and K. Hagiwara for technical assistance in animal breeding and care.

REFERENCES

1. An, P., Sáenz Robles, M. T. and Pipas, J. M. 2012. Large T antigens of polyomaviruses: amazing molecular machines. *Annu. Rev. Microbiol.* **66**: 213–236. [Medline] [CrossRef]
2. Besch-Williford, C., Pesavento, P., Hamilton, S., Bauer, B., Kapusinszky, B., Phan, T., Delwart, E., Livingston, R., Cushing, S., Watanabe, R., Levin, S., Berger, D. and Myles, M. 2017. A Naturally transmitted epitheliotropic polyomavirus pathogenic in immunodeficient Rats: characterization, transmission, and preliminary epidemiologic studies. *Toxicol. Pathol.* **45**: 593–603. [Medline] [CrossRef]
3. Buck, C. B., Van Doorslaer, K., Peretti, A., Geoghegan, E. M., Tisza, M. J., An, P., Katz, J. P., Pipas, J. M., McBride, A. A., Camus, A. C., McDermott, A. J., Dill, J. A., Delwart, E., Ng, T. F. F., Farkas, K., Austin, C., Kraberger, S., Davison, W., Pastrana, D. V. and Varsani, A. 2016. The ancient evolutionary history of polyomaviruses. *PLoS Pathog.* **12**: e1005574. [Medline] [CrossRef]
4. Calvignac-Spencer, S., Feltkamp, M. C. W., Daugherty, M. D., Moens, U., Ramqvist, T., John, R., Ehlers B., Polyomaviridae Study Group of the International Committee on Taxonomy of Viruses 2016. A taxonomy update for the family Polyomaviridae. *Arch. Virol.* **161**: 1739–1750. [Medline] [CrossRef]
5. Dalianis, T. and Hirsch, H. H. 2013. Human polyomaviruses in disease and cancer. *Virology* **437**: 63–72. [Medline] [CrossRef]
6. Ehlers, B., Richter, D., Matuschka, F. R. and Ulrich, R. G. 2015. Genome sequences of a rat polyomavirus related to murine polyomavirus, *Rattus norvegicus* polyomavirus 1. *Genome Announc.* **3**: e00997–e15. [Medline] [CrossRef]
7. Elias, T. and Gaillard, C. B. C. 2000. Common diseases. pp. 106–107. In: The Laboratory Rat Handbook of Experimental Animals (Krinke, G. ed.), Academic Press, London.
8. Gancharova, O. S. and Manskikh, V. N. 2014. Age-related changes in the rat lacrimal gland: Impressive morphology and enigmatic nature. *Russ. J. Dev. Biol.* **45**: 289–298 (in Russian). [Medline] [CrossRef]
9. Gottlieb, K. and Villarreal, L. P. 2000. The distribution and kinetics of polyomavirus in lungs of intranasally infected newborn mice. *Virology* **266**: 52–65. [Medline] [CrossRef]
10. Heuser, E., Fischer, S., Ryll, R., Mayer-Scholl, A., Hoffmann, D., Spahr, C., Imholt, C., Alfa, D. M., Fröhlich, A., Lüscho, D., John, R., Ehlers, B., Essbauer, S., Nöckler, K. and Ulrich, R. G. 2017. Survey for zoonotic pathogens in Norway rat populations from Europe. *Pest Manag. Sci.* **73**: 341–348. [Medline] [CrossRef]
11. John, R., Buck, C. B., Allander, T., Atwood, W. J., Garcea, R. L., Imperiale, M. J., Major, E. O., Ramqvist, T. and Norkin, L. C. 2011. Taxonomical developments in the family Polyomaviridae. *Arch. Virol.* **156**: 1627–1634. [Medline] [CrossRef]
12. Nakanishi, S., Kuramoto, T. and Serikawa, T. 2009. Simple genotyping method using Ampdirect plus and FTA technologies: application to the identification of transgenic animals and their routine genetic monitoring. *Lab. Anim. Res.* **25**: 75–78.
13. Percy, D. H. and Barthold, S. W. 2007. Mouse. pp. 21–23. In: Pathology of Laboratory Rodents and Rabbits (Percy, D. H. and Barthold, S. W. eds.), Blackwell Publishing Professional, Ames.
14. Percy, D. H. and Barthold, S. W. 2007. Rat. p. 127. In: Pathology of Laboratory Rodents and Rabbits (Percy, D. H. and Barthold, S. W., eds.), Blackwell Publishing Professional, Ames.
15. Rigatti, L. H., Toptan, T., Newsome, J. T., Moore, P. S. and Chang, Y. 2016. Identification and characterization of novel rat polyomavirus 2 in a colony of X-SCID rats by P-PIT assay. *MSphere* **1**: e00334–e16. [Medline] [CrossRef]
16. Ward, J. M., Lock, A., Collins, M. J. Jr., Gonda, M. A. and Reynolds, C. W. 1984. Papovaviral sialoadenitis in athymic nude rats. *Lab. Anim.* **18**: 84–89. [Medline] [CrossRef]